DFT Periodic Study of the Adsorption of Glycine on the Anhydrous and Hydroxylated (0001) Surfaces of α-Alumina

ARTICLE *in* THE JOURNAL OF PHYSICAL CHEMISTRY C · NOVEMBER 2007

Impact Factor: 4.77 · DOI: 10.1021/jp0741408

DFT Periodic Study of the Adsorption of Glycine on the Anhydrous and Hydroxylated (0001) Surfaces of α-Alumina

Corinne Arrouvel,† Boubakar Diawara,* Dominique Costa,* and Philippe Marcus

Laboratoire de Physico-Chimie des Surfaces, CNRS-ENSCP (UMR 7045), Ecole Nationale Supérieure de Chimie de Paris, Université Pierre et Marie Curie, 11, Rue Pierre et Marie Curie, 75005 Paris, France

Received: May 29, 2007; In Final Form: August 31, 2007

The adsorption of glycine (G) on the (0001) surfaces of α-alumina with terminations modeling increasing water activity, O_3Al (anhydrous) and (Al_3O-H, O_3Al-OH) (oxy-hydroxide-like) were investigated at low coverage. Different possible glycine conformers have been considered (neutral (NG), zwitterion (ZG), anion (AG)), as well as different binding modes and orientations toward the surface. In all cases, glycine interacts preferentially with the surface through the carboxylic group. The binding with the O_3Al termination of the anhydrous oxide surface may be unidentate Al−O(C) or bridging Al−OCO−Al. The anion perpendicular unidentate form is the most stable one with an energy of adsorption of $\Delta E_{ads} = -214$ kJ/mol. The nature of the Al−O(C) bond is found to be iono-covalent. On the hydroxylated surface with (Al_3O-H, O_3Al-OH) terminations, two types of adsorption may occur: forming only H bonds with the surface ($\Delta E_{ads} = -70$ kJ/mol) or by the combination of Al−OC and H bonds ($\Delta E_{ads} = -159$ kJ/mol). An additional scenario was considered, where glycine substitutes a surface OH group and forms an Al−O−C bond, whereas the OH group combines with a proton from the surface to form a water molecule that coadsorbs with gycine. This reaction is thermodynamically favored ($\Delta E = -213$ kJ/mol). The ZG and AG forms are isoenergetic in a unidentate parallel mode of adsorption. It is shown that coadsorbed water has a stabilizing effect and has an influence on the nature of the most stable G conformer.

1. Introduction

Adsorption of proteins is generally the initial stage in the growth of biofilms on solid surfaces (fouling) in various fields: food industry, marine industry, biomaterial devices. Various types of material surfaces (stainless steel, aluminum alloys, and titanium alloys) as well as a variety of biomolecules are involved.

A better control of the first steps leading to fouling cannot be achieved without a precise knowledge of the nature of the interaction between the biomolecule and the surface. Although numerous works have been performed on the interaction of biological molecules with metal substrates, less work is available on oxide surfaces.

Recently, some model experimental and theoretical works have given insight into the interaction between functions of biological interest and oxide surfaces at the atomic level: glycine was adsorbed on rutile TiO_2 (110),[1−3] silica,[4,5] and Al_2O_3 grown on NiAl(110),[7] and DL-proline was adsorbed on TiO_2 (001).[8] Theoretical studies allow one to obtain detailed data on the nature and strength of the interaction between amino acids and oxide surfaces.[9−14]

Aluminum and aluminum alloys are widely used in the food industry. The surface exposed to water is covered with a hydroxylated Al_2O_3 or AlOOH film, whose structure is often related to be amorphous.[15−19] Al_2O_3 overlayers may also be present at the surface of Ti−Al alloys[20] used in endoprothesis applications[21] and thus be in contact with biomolecules.

α-Alumina is often taken as a reference[22−27] in the studies of transition alumina and other aluminum oxides/hydroxides in which the structure and nature of the surface sites are barely known. Therefore, a number of experimental and theoretical studies have been performed on the basal (0001) α-alumina surface. Its surface structure was studied with LEED, TOF-SARS[28] and its electronic structure with XPS, XAS, and XES.[29−35] Recent reviews summarize those experimental studies.[36−37] Theoretical[38−40] and experimental[41] works have investigated the possible terminations of this surface as a function of the thermodynamic conditions (oxygen and hydrogen chemical potential).

Several terminations for the (0001) surface have been investigated by theoretical works, among others the O_3Al, Al_3O-H,O_3Al-OH, andAl_3O-H,$O_3Al-(OH)_3$.[38−40] They represent the surface under increasing water activity. The first termination is found on a cleaved surface under UHV, the second one exhibits an oxihydroxide-like termination (AlOOH), whereas the latter termination is rather trihydroxide-like ($Al(OH)_3$). The latter termination is reported to be the most stable one under a wide range of thermodynamic conditions,[35,40] and the AlOOH one may be stabilized under low water activity conditions.[28,29,31]

Glycine (NH_2CH_2COOH) is the smallest aminoacid (AA) and exhibits both reactive functions COOH and NH_2 (Figure 1). With its small size, it allows exhaustive studies of its adsorption on surfaces with theoretical tools at reasonable computational cost.

We present here a periodic DFT study of the adsorption of the simplest aminoacid, glycine, (G) on (0001) α-alumina surfaces exhibiting O_3Al and Al_3O-H,O_3Al-OH terminations. The choice of these terminations is motivated by three reasons:

* Corresponding authors. E-mail: dominique-costa@enscp.fr; bob-diawara@enscp.fr. Tel: + 33(0)1 44 27 67 27. Fax: + 33(0)1 46 34 07 53.

† Present address: Department of Chemistry, University of Bath, BATH, BA2 7AY, UK.

10.1021/jp0741408 CCC: $37.00
Published on Web 11/10/2007

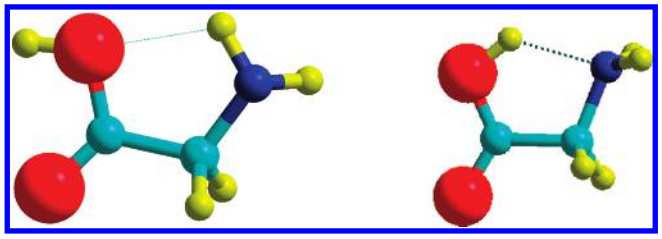

Figure 1. Optimized geometries of neutral (NG) glycine as in the gas phase (a) NG-I glycine; (b) NG-II glycine. Red, O; yellow, H; light blue, C; dark blue, N atoms.

first, we gradually increase the water activity at the interface; second, both terminations exhibit undercoordinated surface Al cations, which may form strong bonds with the carboxylate group of glycine; third, the Al_3O-H,O_3Al-OH termination represents a simple model for the hydrated thin films on aluminum alloys. We believe that the understanding of a simple model interface is a starting point for further gradual increase of the complexity and for future comparison with other, more complex systems.

The paper is organized as follows: the O_3Al and Al_3O-H,O_3Al-OH terminations of the α-alumina (0001) surface and the structure of neutral glycine (NG) isomers are presented, and the results are compared with previous ones. Then, the glycine/alumina interaction is analyzed using Bader charge and projected density of state (PDOS). In the present study, we restrict the investigation to low glycine coverage.

2. Methodology

2.1. Periodic DFT Calculations. Total energy calculations were performed within the density functional theory (DFT) and the generalized gradient approximation (GGA) of Perdew and Wang.[42] GGA is well adapted to the study of oxides because it improves cohesive energies.[43] To solve the Kohn−Sham equations, we use the Vienna ab initio simulation package (VASP).[44−46] VASP performs an iterative diagonalization of the Kohn−Sham Hamiltonian via unconstrained band-by-band minimization of the norm of the residual vector to each eigenstate and via optimized charge density mixing routines. The convergence criterion for the electronic self-consistent cycle is fixed at 0.1 meV per cell. The eigenstates of the electron wave functions are expanded on a plane-waves basis set using pseudopotentials to describe the electron−ion interactions within the projector augmented waves (PAW) approach.[47] For total energy calculations, we use a cutoff energy of 300 eV with O soft pseudopotentials. These calculation conditions have given very reasonable results, including good agreement between computed and experimental OH stretch frequencies in recent works.[48] We verified on the main results that the scale of the energies of adsorption obtained with a soft potential is maintained when a normal O potential is used. The optimization of the atomic geometry at 0 K is performed by determining the exact Hellmann−Feynman forces acting on the ions for each optimization step and by using a conjugate gradient algorithm until the geometric convergence criterion on the energy (1 meV/cell) is reached. A convergence on the *k*-point mesh is also reached. We include the dipolar moment along the *z* axis because the glycine molecule is adsorbed on one surface of the slab only. Charge calculations were performed using the Bader theory.[49,50] As suggested by Bader, atomic charges are calculated using the decomposition of electronic charge density into atomic contributions by dividing the space into atomic regions with surfaces at a minimum in the charge density. We have used the "Bader" code developed by Henkelman et al. and based on their recently proposed fast algorithm,[51] which assigns each point on a regular (*x*, *y*, *z*) grid to one of the regions by following a steepest ascent path on the grid. The grid used was 160 × 160 × 560.

For DOS calculations, we performed a single point calculation at a cutoff energy of 400 eV, without any smearing addition and with an increased precision on the *k*-point grid. The Wigner Seitz radii of Al and O were adjusted with the bulk alumina to 1.0 and 1.43 Å, respectively.

For molecular dynamics calculations, the atom positions and cell dimensions were relaxed at constant temperature (300 K). The time step was set at 1.5 fs, and the geometries are sampled up to 2 ps to have a reliable image of the equilibrium geometry at 300 K using a micro-canonical ensemble.

All of the starting and resulting configurations as well as the DM movies were visualized with the Modelview software.[52]

2.1.1. Bulk Oxide. The rhomboedral ($R\bar{3}c$) unit cell of α-alumina, according to X-ray data,[53] was taken as the starting point for the calculations of the bulk oxide. We used the GGA-PW91 functional with PAW pseudopotential, as already performed successfully in previous theoretical works on α-alumina.[23,25,27,40,54]

The *k*-point grid was optimized with tests *k* points grids of (4 × 4 × 4), (5 × 5 × 5), and (6 × 6 × 6). Finally, a 6 × 6 × 6 grid was used. Alternate calculations with relaxation of the cell volume on one side and of the cell shape and ions positions on the other side were performed until the final stability was reached. The geometry optimization is carried out by calculation of the Hellmann−Feynman forces and an energy convergence criterion of 3 meV.

2.1.2. Oxide Surface. We consider an area of the monoclinic supercell (2 × 2) large enough to adsorb glycine at low coverage without lateral interactions. The (2 × 2) surface corresponds to a surface area of 79.87 Å^2 with $a = b = 9.60$ Å. The *k*-point mesh is (3 × 3 × 1) in order to keep the same calculation level as that used when studying the bulk. The number of oxygen layers is 6, the slab thickness is 11 Å, and the vacuum thickness has been chosen thick enough (∼18 Å) to avoid interactions between 2 slabs along the *c* direction. A full relaxation of the ions with fixed cell parameters was performed.

The surface energy in vacuum, Γ^0_{hkl}, for a given (*hkl*) crystal orientation, was calculated using formulas already described in the literature.[48] We did not perform a systematic study of the (0001) surface energy convergence because this was performed in previous theoretical works: Hector et al., in their study of (0001) α-Al_2O_3,[54] mention that 5−7 O layers must be used in order to converge the surface energy, with the same method used (VASP, PW91, PAW). Wang et al.[39] uses 6 O layers with a similar theoretical method. Ruberto et al.[27] mention that with the same method (PW91, PAW) energy surface convergence is achieved for $n = 4$ O layers.

To hydroxylate the surface, one water molecule per surface Al_{III} (Al tricoordinated) atom is added, forming one OH monocoordinated to an Al (μ_1−OH) becoming tetracoordinated ($Al_{IV}-\mu_1-OH$) and one OH tricoordinated to three Al_{IV} atoms (μ_3−OH). Again, a full optimization was performed.

2.1.3. Glycine. We have included a glycine molecule in a squared box with 20 Å on each cell parameter. The *k*-point grid is (1 × 1 × 1). All of the atoms in the molecule are left free to relax. The glycine taken as a starting point is an isolated neutral molecule that represents glycine in the gas phase, which may coexist under the form of the NG-I and NG-II conformers (see Figure 1).[55,56] Other conformers may be stabilized on the

alumina surface, as the NG-II, the zwitterion (ZG), and the glycinate anion (AG) forms.

2.1.4. Glycine/Alumina Interaction. The different configurations of glycine adsorbed on the surface are referred to NG, ZG, or AG. The surface coverage considered was 1.25 G/nm^2, which represents a low surface coverage case (for comparison, glycine in a plane of solid α-glycine has a density of 4 G/nm^2). The atoms of the three Al and O upper layers, as well as the OH groups and glycine atoms, are fully relaxed.

To study the glycine/alumina interaction, we considered and tried to answer the following questions:

Which of the two chemical functions (COO(H)/NH_2(H)) is the most reactive?

Does glycine bind with Lewis sites or does it form only H bonds?

In case of the formation of an Al-carboxylate bond, is the bonding mode monodentate, bidentate, or bridging?

Are there possibilities to combine the Al−carboxylate bond and H bonding?

Are there proton transfers from glycine to the surface or from the surface to glycine?

What are the preferred orientations of glycine to the surface?

2.2. Relative Energy Calculations. The energies of interaction/adsorption of glycine (G) on the surface were calculated considering the reaction

$$NG^{gas} + \text{alumina} \rightarrow (\text{G, alumina}) \quad (1)$$

where NG^{gas} is the reference neutral glycine conformer in the gas phase, thus using the formula

$$\Delta E_1 = \Delta E_{ads} = E(G, \text{alumina}) - E(NG^{gas}) - E(\text{alumina}) \quad (1')$$

where $E(NG^{gas})$ and E(alumina) are the total electronic energies of the glycine (neutral) and alumina surface (either anhydrous or hydroxylated), obtained after separate geometry optimizations, and $E(G,$ alumina) is the total electronic energy of glycine in interaction with the alumina surface.

We also calculated an overall energy for the reaction

$$Al_3O{-}H,O_3Al{-}OH + NG \rightarrow Al_3O,O_3Al{-}G{-}H_2O \quad (2)$$

where the glycine molecule substitutes a μ_1−OH group; this μ_1−OH group was recombined with a surface Al_3O−H proton in a water molecule coadsorbed with glycine at the surface. This time, the energy of reaction

$$\Delta E_{subst} = E(Al_3O,O_3Al{-}G{-}H_2O) - E(NG^{gas}) - E(Al_3O{-}H,O_3Al{-}OH) \quad (2')$$

combines the energy of adsorption of glycine from the gas phase, the energy of recombination of a water molecule starting from two OH groups, and the energy of adsorption of this water molecule on the hydroxylated surface.

The total energies of the different glycine conformers in interaction with the alumina surface were also compared, and ΔE_{conf} was estimated as the difference in energy between a given conformers and the most stable one: $\Delta E_{conf} = E(\text{conf}) - E(\text{most stable conf})$ (kJ/mol); defined in this way, ΔE_{conf} is always a positive value.

3. Results

3.1. Alumina. *3.1.1. α-Alumina Bulk Structure.* All Al layers of the rhomboedral structure consist of hexagonal arrangements of atoms, occupying octahedral sites (Al_{VI}). The optimized cell parameters are reported in Table 1, together with the experimental ones and those calculated by Hector et al. under the same formalism (GGAPW91 and PAW), with a higher cutoff energy (700 eV).[54] The results presented here fit the experimental values as well as those obtained in ref 54. There are two Al−O distances in the bulk, calculated as 1.872 and 1.989 Å (see Table 1).

TABLE 1: Calculated (VASP) versus Experimental Structural Parameters of α-Alumina

α-Al_2O_3	experimental	calc. ref 54	calculated (bulk) (this work)	calculated (0001) (this work)
$a = b$	4.759(7)[53]	4.82	4.80	fixed to the bulk value
c	12.993(5)	13.16	13.114	fixed to the bulk value; (19 Å vacuum)
V (Å^3)	254.93		261.88	
Al−O_1	1.853		1.872	1.868 underneath the (0001) surface
Al−O_2	1.974		1.989	1.926 underneath the (0001) surface

3.1.2. (0001) Surface of α-Al_2O_3. 3.1.2.1. O_3Al Termination: Anhydrous Surface. Tasker's rule predicts that the (0001) α-alumina surface is terminated by half of an Al layer.[57] Results of first-principles calculations agree with this.[28,39,58] The surface Al atoms relax within the plane of oxygen atoms, as shown in Figure 2. The surface Al atoms are threefold coordinated (Al_{III}); their density is 8.7 Al_{III}/nm^2. Our calculations show that this surface has a surface energy of 1.66 J/m^2, a result in agreement with Ruberto et al.[27] (1.60 J/m^2). The Al−O bond lengths underneath the first layers are near that of the bulk (see Table 1), showing that the thickness of the slab is large enough to reproduce bulk properties.

The Al_{III}−Al_{III} distance at the surface is 4.80 Å. Each Al_{III} is surrounded by six Al_{III} at equivalent distances in an hexagonal network (see Figure 2a). The Bader charge analysis shows that the Al charge at the surface (2.41) is not significantly changed as compared to the Al in the inner layer (+2.46), as a result of the relaxation of the Al ion into the oxygen plane. The same is observed for the O ions, which bear charges of −1.62 and −1.63 at the surface and in the bulk, respectively. The surface AlO_3 plane has a negative charge of −2.45 per AlO_3 unit.

3.1.2.2. $Al_3O{-}H,O_3Al{-}OH$ Termination: Surface Hydroxylation. The Lewis acid surface sites (Al_{III}) are very reactive toward H_2O, and first-principles calculations predict that the surface is hydroxylated even at low water activity.[38,40] In the $Al_3O{-}H,O_3Al{-}OH$ termination, each Al atom of the surface now bears one OH group, and an additional proton binds a O surface atom. Thus, one obtains a monolayer (ML) of 8.7 Al_{IV}−μ_1OH (Al−OH)/nm^2 and 8.7 μ_3OH (Al_3−OH) /nm^2. The experimentally measured adsorption energy for water[53] lies between −96 and −172 kJ/mol. Our calculated adsorption energy (−166 kJ/mol) for the OH monolayer is similar to previously calculated values (−146 kJ/mol).[58] The charge of the Al atoms bearing the terminal OH groups is now 2.43, a value in between the charge of the Al at the dry surface (2.41) and the sixfold coordinated Al ions under the surface (2.46). The surface OH plane has a negative charge of −1.65 per AlO_3,H_2O unit.

3.2. Glycine. Glycine ($NH_2{-}CH_2{-}COOH$) is neutral in the gas phase, without local charges on the functional amino and carboxylic groups (see Figure 1). The relative stability of the two most stable conformers NG-I and NG-II might depend on the quality of the calculation.[55,56] We found that type NG-II is more stable by 5 kJ/mol than type NG-I at a cutoff energy of 300 eV and by 2 kJ/mol at a cutoff energy of 700 eV. Accurate

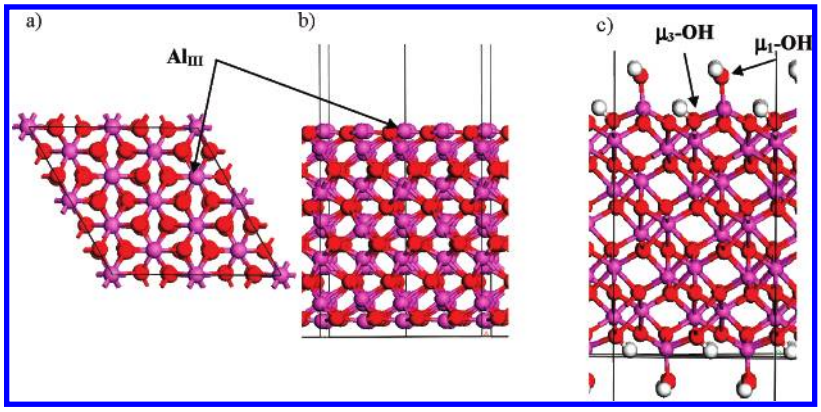

Figure 2. (2 × 2) (0001) α-Alumina slab used to model the alumina surface: (a and b) O_3Al termination: (a) top view; (b) side view; after geometry optimization, the Al atoms have relaxed in the plane of the oxygens; (c) Al_3O-H,O_3Al-OH termination, hydroxylated alumina, side view. Pink, Al; red, O; white, H.

TABLE 2: Configurations and Energies of Adsorption (ΔE_{ads}) (kJ/mol) Calculated for Glycine through the COO(H) Moiety on the O_3Al Termination of the α (0001) Surface at Low Coverage[a]

	binding mode of COO(H) to aluminum cation		
conformer	unidentate	bidentate	bridging
NG	NI-153 (perp)(3b) NI-132 (tilt)(3c) NII-94 (perp)(3e)	unstable (perp)	NII-33 perp
AG	**−214** (perp)(3f) para: unstable, turns ZG spontaneously	−159 (perp)(3h)	**−194** para (3g) −153 perp
ZG	**−187** (para) (3d) perp: unstable, turns NG spontaneously	unstable (para)	unstable (perp and para)

[a] The corresponding structures are depicted in Figure 3 and their labels are shown in parentheses.

calculations at the MP2 level have shown that conformer I is more stable by 2.2 kJ/mol than conformer II.[59] Thus, our calculations differ by less than 10 kJ/mol from more accurate methods, which is an acceptable result. The type NG-II will be used for our energy reference for the glycine in gas phase. Both conformers have negative charges of −0.1 to −0.18 on the COOH end and positive charges of +0.30−0.32 on the NH_2 end. The oxygen atoms bear charges of −1.1−1.2. The zwitterion form (ZG) (not shown) exhibits a negative charge of −0.68 on the COO^- end with a charge of −1.17 on O atom and a positive charge of +0.38 on the NH_3^+ end.

3.3. Adsorption of Glycine on Alumina. Different forms of adsorbed glycine (neutral, anion, zwitterion)[60] have been tested, and different orientations to the surface (parallel and perpendicular) as well as different types of bonds (Al−OC bonds, hydrogen bonds) have been considered. We will describe the most stable structures obtained and analyze the influence of the alumina surface hydroxylation state on the adsorption modes. The main results for the anhydrous surface are summarized in Table 2 and Figure 3 and in Table 3 and Figure 4 for the hydroxylated surface.

3.3.1. Glycine Interaction with Anhydrous Alumina O_3Al. Starting from neutral glycine NG, we first investigated which terminal function interacts mostly with the O_3Al surface. The interaction of NG-II with the Al_2O_3 surface through the NH_2 terminal group leads to the formation of an Al−N bond (Al−N = 2.017 Å) with an energy of adsorption of ΔE_{ads} = −110 kJ/mol (N-II) (Figure 3a). For the interaction of the COO(H) function with the alumina surface, we investigated different modes of $O_3Al-OOC$ binding, unidentate, bidentate, and bridging modes, and two orientations, parallel and perpendicular to the surface. We also considered the possibility of a proton transfer from the COOH moiety either toward the surface, resulting in the stabilization of the anionic (AG) species, or to the NH_2 one, resulting in the zwitterion (ZG) conformer. All initial configurations involved one or several Al−OC bond(s) (Figure 3b−h).

3.3.1.1. Neutral Glycine. Neutral glycine (NG) is stabilized on the alumina surface in all configurations considered except the bidentate configuration. The most favorable configuration (ΔE_{ads} = −153 kJ/mol) is obtained for the unidentate, perpendicular NI conformer (Figure 3b and Table 2). The glycine molecule binds with one Al atom, with an Al−O bond length of 1.84 Å, and the carbonyl moiety makes H bonds with two surface oxygens (with H···O bond lengths of 2.16 Å). Starting from a parallel orientation, a tilted configuration is stabilized (Figure 3c, Table 2) because the basic NH_2 function does not tend to form bonds with the basic surface oxygens. The Al−OC bond length is of the same order (1.88 Å), and the carboxyl moiety makes one H bond with a surface oxygen (1.63 Å). The perpendicular orientation is more stable by 21 kJ/mol than the tilted one, although the number of hydrogen bonds is lower.

The bridging mode of binding is only slightly exothermic (ΔE_{ads} = −30 kJ/mol), the adsorption energy being on the order of magnitude of a H bond.

3.3.1.2. Zwitterion. The zwitterion form is stabilized only in the unidentate configuration, in a parallel orientation (ΔE_{ads} = −187 kJ/mol), with the acid NH_3^+ function forming two H bonds with surface oxygen atoms (Figure 3d). In the unidentate perpendicular orientation, the ZG form is not stable and a proton-transfer spontaneously occurs from the NH_3 moiety to the CO one, resulting in the NII configuration (Figure 3e). The same trend is observed for the bridging mode of adsorption: the zwitterion is not stable and turns spontaneously into the anionic form. Similarly, the bidentate mode of adsorption is not stable and turns into the unidentate one.

3.3.1.3. Anion. The glycinate anion is stabilized in a unidentate perpendicular configuration, with an adsorption energy of ΔE_{ads} = −214 kJ/mol (see Figure 3f); it interacts similarly to the neutral form NG, and a proton has been transferred from the carboxyl group to alumina surface oxygen (μ_3O). The Al−O(C) distance is 1.81 Å. The bridging parallel configuration (Figure 3g) is slightly less stable (ΔE_{ads} = −194 kJ/mol) than the perpendicular unidentate one (see Table 2), whereas the bridging perpendicular configuration is the less stable (ΔE_{ads} = −153 kJ/mol, not shown). In the bridging mode, the Al−O bond lengths are 1.94 and 2.04 Å. On this surface, the Al−Al

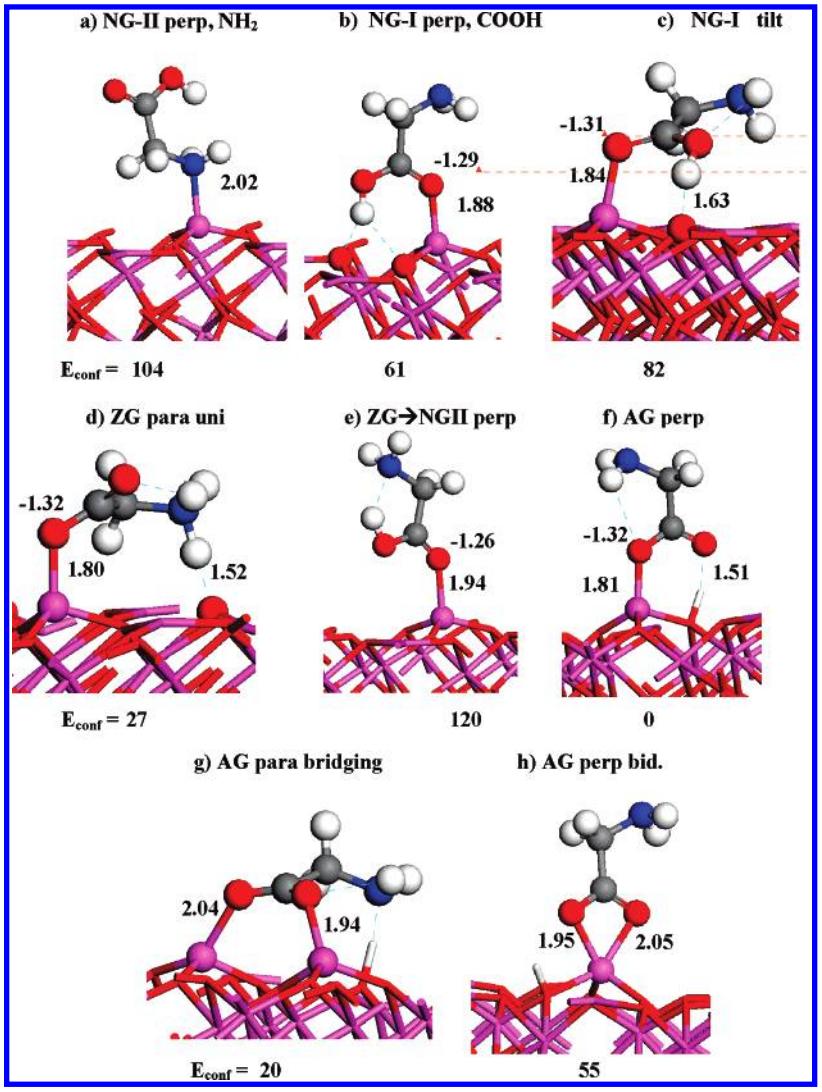

Figure 3. Optimized configurations of the different stable forms (neutral (NG), zwitterionic (ZG), anionic (AG)) of glycine on O_3Al alumina termination and energies relative to the most stable form (E_{conf}); the energies of adsorption ΔE_{ads} (kJ/mol) are reported in Table 2. Distances are reported in angstroms.

TABLE 3: Configurations and Energies of Reaction (ΔE_{subst}) (kJ/mol) Calculated for Glycine in Different Forms (NG, ZG, AG) on the Al_3O-H, O_3Al-OH (0001) Surface at Low Coverage[a]

		binding mode to Al_{IV}	binding mode to Al_{III}	
conformer	H bonds only	unidentate	unidentate	bridging
NG	−65 perp (4a) −58 para (4b)			
ZG	−70 para (4c) perp not stable	unidentate −159 (4d)	−203 (4e)	not stable
AG	unstable, turns ZG spontaneously	bridging not stable unidentate −107	−213 (4f)	not stable

[a] The corresponding structures are depicted in Figure 4 and their labels are shown in parentheses.

distance is rather long (4.80 Å), which explains why the bridging configuration (formation of two Al−OC bonds) is not favored over the unidentate one. In the unidentate parallel orientation, the anion form is not stable and turns into the ZG unidentate parallel one. It is interesting that the reactivity of the NH_3^+ moiety depends on the binding mode of the carboxylate end: indeed, in the orientation parallel to the surface, the AG unidentate form is not stable and turns into the ZG form (Figure 3d), whereas the reverse is observed with the bridging mode (spontaneous proton transfer from ZG to the surface, resulting in the AG form (Figure 3g)). The bidentate configuration is stabilized, with an energy of adsorption of $\Delta E_{ads} = -159$ kJ/mol, due to the interaction between the Al_{III} Lewis acid and the negatively charged glycinate (Figure 3h). However, this mode of binding remains less stable than the unidentate and bridging ones.

To summarize, there are interdependent relationships between the mode of binding/orientation to the surface and the stability of the glycine conformer: a unidentate binding favors the anionic form perpendicular to the surface and the zwitterion form parallel to the surface, whereas a bridging binding favors the anionic form in a parallel orientation. Finally, the most stable configuration is the anion perpendicular form.

3.3.1.4. Charge Distribution. The Bader analyses of NG, ZG, and AG adsorbed on anhydrous alumina surface were performed. We observed that the charge of the glycine O bonded

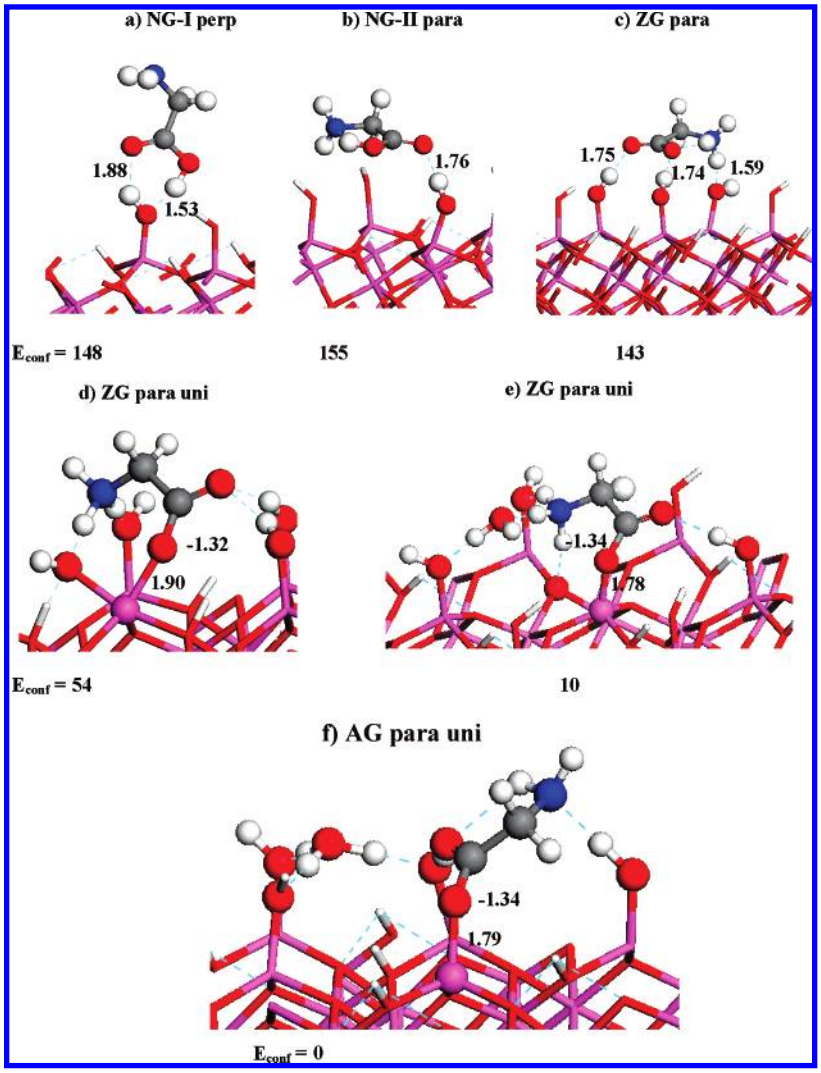

Figure 4. Optimized configurations of the different stable forms (AG, ZG, NG) of glycine on the Al_3O-H,O_3Al-OH alumina termination, energies relative to the most stable form (E_{conf}); (a−c) glycine in interaction with hydroxyls only; (d) bond to an Al_{IV}; (e and f) bond to an Al_{III} with coadsorption of a water molecule (e) or a solvated proton (f, insight). The energies of adsorption ΔE_{ads} are reported in Table 4. Distances are reported in angstroms.

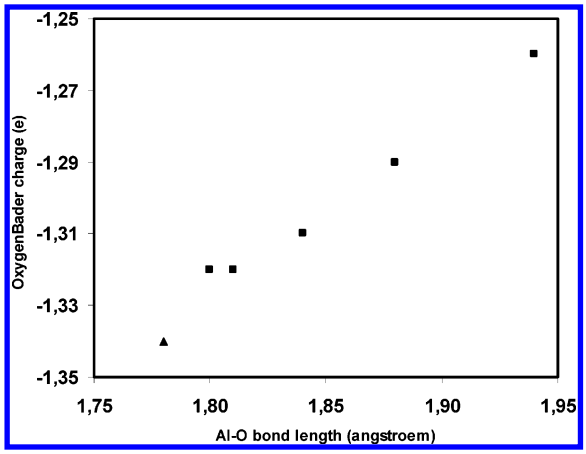

Figure 5. Correlation between the charge of the oxygen atom of glycine bond to Al and the Al−OC bond length (in Å). ■, glycine on anhydrous alumina; ▲, glycine on hydroxylated alumina.

to Al is slightly more negative (0.15−0.20 more electron) than that in free glycine, whereas the Al ion charge is altered by less than 0.05 e). This charge is linearly related to the Al−O bond length, as illustrated in Figure 5. We also noted a relationship between the Al−O bond length and the energy of adsorption: (i) configurations 3f and 3d are the most stable with an Al−O bond length near 1.80 Å, (ii) configurations 3b and 3c have intermediate stability with a bond length around 1.86 Å, (iii) configuration 3e is the less stable with an Al−O bond length of 1.94 Å.

No charge transfer occurs between the surface and glycine adsorbed in the NG or ZG form, but the increase of the O charge is compensated in the glycine backbone by an increase of the C positive charges.

For the AG form, there is a net negative charge transfer (−0.8*e*) from the surface to glycine, due to the proton transfer from glycine to the surface. We observed no noteworthy influence of the mode of adsorption (unidentate (3f), bridging (3g), and bidentate (3h)) on the charges of the O atoms of the COO end and on the Al charge.

3.3.1.5. Electron Density of States. The nature of the Al−O(C) bond (either purely ionic or iono-covalent) was investigated for the most stable configuration obtained (shown in Figure 3f) by means of electronic analysis. Figure 6 shows the density of states (DOS) projected on Al and O of the bulk oxide (6a), and on the Al−O(C) atoms involved in the glycine−surface bonding (Figure 6b). The valence band shown in Figure 6a is composed of mainly oxygen 2p orbitals. An aluminum contribution is identified, suggesting that the O−Al bond in α-alumina tends to be more iono-covalent than purely ionic. Similar results

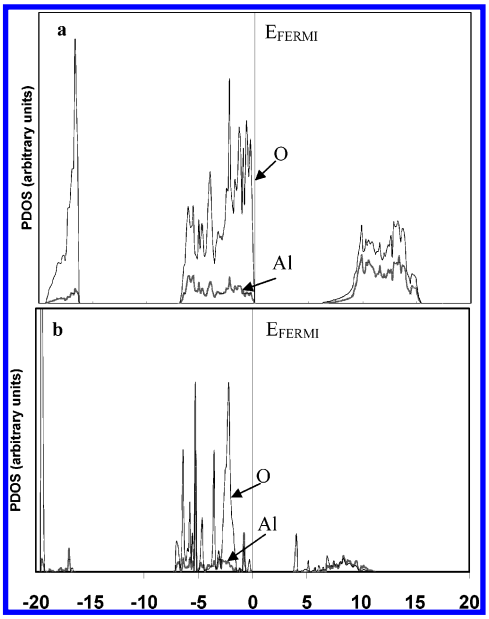

Figure 6. Projected density of states (PDOS, arbitrary units) on Al and O in (a) the α-alumina bulk and (b) involved in an Al−O(C) bond between glycine and the anhydrous alumina surface (configuration shown in Figure 3f). Fine line, O projected DOS; bold line, Al projected DOS.

were obtained in the case of γ-alumina.[61] The same trend is also observed with the projected DOS on the Al−O(C) in the case of the adsorbed glycine molecule (Figure 6b): the bond formed is not purely ionic but still contains a covalent character. Other ab initio results obtained for $(Al-OCOH)^{3+}$ complexes in vacuum concluded with a covalent contribution of 31% for this unidentate complex via a natural bond order (NBO) analysis.[62] However in the $(Al-OCOH)^{3+}$ complex, the Al ion is not involved in other bonds as in the present study, where the surface Al ion has three other Al−O bonds. The nature of the Al−OC bond of glycine adsorbed on the alumina surface will be investigated in more details in a forthcoming paper.[63]

3.3.2. Interaction of Glycine with the Al_3O-H,O_3Al-OH Termination. On the hydroxylated surface, glycine can bind to the surface through a H-bond network, or a combination of H bonds and Al−OC bonds, as detailed hereafter. Because the study on the anhydrous surface lead to the conclusion that bidentate adsorption is not stable, we restrained our study to unidentate and bridging modes of adsorption. Table 3 summarizes the obtained results.

3.3.2.1. Adsorption through a H bond network.

3.3.2.1.1. Neutral Glycine. The adsorption of neutral glycine NG in perpendicular and parallel orientations to the surface with the formation of H bonds with surface hydroxyls was investigated (Figure 4a and b). They are nearly isoenergetic, with an energy of adsorption around $\Delta E_{ads} = -60$ kJ/mol, corresponding well to the formation of H bonds. For both modes of adsorption, glycine forms H bonds with μ_1−OH groups only because the μ_3−OH groups are not available for making H bonds with glycine because of their location under the μ_1−OH groups. Such a trend was already observed in theoretical studies of adsorption of pyridine on the hydroxylated γ-Al_2O_3 surface.[64]

In the perpendicular mode of adsorption, NG-glycine is bonded to the surface via two H bonds with μ_1−OH groups; the most stable structure is obtained for the NG-I form in interaction with one μ_1−OH group, forming a ring C−O−H−O−H−O similar to the glycine dimer (Figure 4a). Such a configuration was already observed in a previous work on the interaction of glycine with one isolated hydroxyl group on silica.[5] The OH group is both H-donor and H-acceptor. It is interesting to note that the binding of glycine to one single OH group is energetically more favorable than to two vicinal OH groups, by nearly 30 kJ/mol (figure not shown).

3.3.2.1.2. Zwitterion. As for the anhydrous surface, the ZG form is not stable in the perpendicular orientation and leads spontaneously to the NG-II form. In the parallel orientation to the surface, the ZG form may be stabilized (Figure 4c) and is, in this case, slightly more stable ($\Delta E_{ads} = -70$ kJ/mol) than the NG form ($\Delta E_{ads} = -58$ kJ/mol). We conclude that both the ZG and NG forms may be stabilized on the hydroxylated alumina surface and that we obtain no evidence of an unequivocal tendency of μ_1−OH groups of the α-alumina surface to solvate glycine.

3.3.2.1.3. Anion. The anion form is not stabilized by a H-bond network and turns spontaneously to the ZG form.

3.3.2.2. Combination of Al−OC Bonds and H Bonds. Here we focus on the ZG and AG forms, which are stabilized by the formation of an Al−OC bond on the hydroxyl-free surface. We first studied the possibility of a combination of binding with an hydroxylated Al_{IV} atom and of H bonds with OH groups. The adsorption energy in the ZG form is higher than when forming only H bonds and reaches $\Delta E_{ads} = -159$ kJ/mol (Figure 4d). The Al_{IV}−OC bond length is 1.89 Å, a bond length corresponding to that of Al−O in the bulk, confirming that a strong bond has been formed. This bond has been formed at the expense of the Al−O(H) bond because the μ_1−OH group attached to the Al atom has now a longer Al−O bond length (1.93 instead of 1.73 Å before adsorption).

The anionic form is also stabilized, but this form is less stable than the ZG form ($\Delta E_{ads} = -107$ kJ/mol, not shown in the Figure 4).We note the role of the basic μ_1−OH groups, which are proton acceptors, and thus may stabilize the AG form in a parallel unidentate adsorption. Such a stabilization was not observed on the surface μ_3−O anions.

Finally, the substitution of one μ_1−OH group by the carboxylate function of glycine, with the formation of an Al_{III}−OCO bond was considered. The free OH group was recombined with a proton from the surface to form a water molecule that was located in a H-bond network of OH groups (see Figure 4e and f). The calculated enthalpies of reaction (ΔE_{subst}) are negative, indicating an exothermic process of hydroxyl displacement from the surface. The most stable conformation is obtained for glycine in a parallel configuration, where an Al_{III}−OC bond and three additional H bonds with μ_1−OH groups are formed (the perpendicular conformation being 55 kJ less stable because only one H bond is formed (not shown)). The Al_{III}−OC bond has a bond length of 1.79 Å, 0.1 Å shorter than the corresponding Al_{IV}−OC bond formed with an hydroxylated Al atom. The anionic form (Figure 4f) and the zwitterions form (Figure 4e) may be considered as isoenergetic, with an energy of reaction $O_3AlOH + NG \rightarrow O_3Al-Gly + H_2O_{ads}$ of, respectively, $\Delta E_{subst} = -213$ and -204 kJ/mol. This points out the role of the coordination number of the Al atom, and thus of the strength of the Al−OC bond, on the proton transfer from amine to the surface: indeed, an Al_{IV}−OC bond does not favor the AG form (which is less stable than the ZG form), whereas an Al_{III}−OC bond renders the AG and ZG forms isoenergetic. This result shows some similarity with that on the anhydrous surface, likely because the coordination number of the Al_{III} atom is the same. In the anionic configuration, a proton has been transferred to an adsorbed water molecule, forming an "OH-solvated H_3O^+" species on the surface (see Figure 4f); this configuration was

found stable in a molecular dynamics (MD) run of 0.6 ps at 300 K. The coadsorbed water molecule plays also a role in the stabilization of the anionic form. Indeed, a geometry optimization performed in the absence of this water molecule leads to the spontaneous reformation of the zwitterion form. Thus, the anionic form may be stabilized through a complex interplay of an Al−OC bond and additional H bonds between OH groups and water molecules.

In the ZG configuration, the adsorbed water molecule interacts with the NH_3 moiety and one OH group. The energy of interaction of water with the surface and the glycine molecule is −103 kJ/mol,[65] a value somewhat higher than what is expected for water chemisorbed on OH groups. (The energy of adsorption of water on hydroxyl groups was calculated to be −75 kJ/mol, a value near the value of 80 kJ/mol obtained by other authors for the formation of one ML of molecular water on the Al_3O-H,O_3Al-OH termination.[40]) This higher energy of interaction suggests the stabilizing effect of water and glycine coadsorption on the surface.

Bridging $Al_{III}-OCO-Al_{IV}$ configurations were also investigated. The results show that these configurations are not stable, turning spontaneously in a unidentate mode adsorption on the Al_{III}. Here, the Al_{IV} atoms are not able to bind a second strong bond with the carboxylate moiety.

3.3.2.3. Charge Distribution. When glycine is adsorbed through hydrogen bonds, there are no changes in the O or C charges. In contrast, when glycine is adsorbed through a Al−OC bond, the charge of the O atom increases by 0.15−0.25, as observed on the anhydrous surface. Again, this charge increase is not due to a surface−glycine electron transfer, which remains negligible but rather to an electronic reorganization in the glycine molecule. For the anionic form, the charge transfer is due to the proton transfer from the glycine molecule to the surface.

4. Discussion

On anhydrous alumina surfaces, the present results suggest that glycine adsorption is driven by the formation of Al−OC bond(s). More complex events are evidenced on the hydroxylated surface because adsorption may occur either through only H bonds or through a cooperation between one Al−OC bond and a H-bond network involving surface OH groups and adsorbed water.

To our knowledge, there is only one published experimental work on glycine adsorption on an anhydrous alumina surface.[7] In this study, glycine was adsorbed at 110 and 300 K on Al_2O_3/NiAl(110). The glycine monolayer (ML) was composed essentially of a mixture of ZG and AG at 110 K and of ZG at 300 K. The glycine ML desorbed at 350 K, that is, only 50 K above the temperature of multilayer desorption, a temperature that suggests a rather weak energy of adsorption of glycine with the surface. In our case, in contrast, we calculated a rather high energy of adsorption of glycine on the anhydrous alumina surface (−214 kJ/mol), due to the Al−OC bond. A calculation of the temperature of desorption of glycine from the surface was performed in taking into account the Gibbs free energy of glycine in the gas phase as performed in a previous work,[13] using a formalism described in ref s 39 and 40: Considering that glycine adsorbed in multilayers has an energy of adsorption similar to the cohesive energy in bulk α-glycine (calculated as −103 kJ/mol with VASP), and taking a glycine partial pressure during the TPD experiments of $P/P^\circ = 10^{-9}$, glycine multilayer desorption is calculated to occur at 250 K (to be compared with 300 K experimentally measured), whereas glycine adsorbed through an Al−OC bond on the alumina surface should desorb at 475 K, thus at a temperature 175 K higher than the multilayer. This calculation confirms that the binding energy of glycine adsorbed on Al_2O_3/NiAl(110) (desorbing at 350 K) is less than that calculated here for glycine on anhydrous α-Al_2O_3. Indeed, the Al_2O_3/NiAl(110) surface cannot be directly compared with the α-(0001) Al_2O_3 surface. The Al_2O_3/NiAl(110) is oxygen-terminated and thus does not exhibit Al atoms at the free surface. Despite this lower energy of interaction, it is interesting that the conformers identified at low temperature (110 K) below and at the ML coverage are anionic forms, in agreement with our own results. The authors propose an electrostatic interaction between the carboxylic oxygen and the Al cations underneath the surface O layer, which is not in disagreement with our results, but could rather complete it and again highlight the role of the Al surface cations. In their model, the screening of the O layer may decrease the strength of the electrostatic interaction and can explain the higher interaction energy we have obtained with a model with a direct interaction between the carboxylic oxygen and the Al cations.

On hydroxylated/hydrated aluminum surfaces (exposed to water), or aluminum oxide/hydroxide surfaces, experimental works on organic acids report a weak interaction (outer sphere adsorption) on hydroxyls groups[66−68] and/or the adsorption on low coordinated Al ions (inner sphere adsorption)[69−72,73] depending on the experimental conditions. In the present work, we obtained an energy of adsorption of glycine of around 70 kJ/mol by combined interaction of the carboxylate and amine moiety with surface OH groups by hydrogen-bond network, that can be compared with experimental results, where rinsing is observed to remove the adsorbed carboxylate groups.[69] The role of the OH groups in this mode of adsorption was unambiguously evidenced in ref 69 as the amount of adsorbed matter increases with the OH concentration at the surface of the oxidized aluminum.

On coordinatively non-saturated Al surface atoms, (as is the case here even for the $O_3Al_{IV}HOH$ termination), we showed that an Al−OC bond may be formed, the strength of which increases with decreasing coordination number of Al (from IV to III), inducing a much higher energy of adsorption (from 160 to 200 kJ/mol) of glycine with the surface than when forming only H bonds.

All the studies converge to conclude that on the one side, surface hydroxyl groups are responsible of a low energy of adsorption (outer sphere adsorption), and, on the other side, strong (inner sphere) adsorption may occur on Al surface atoms, depending on their coordination number.

The data reported here show that the unidentate mode of adsorption is the most stable one (more stable than the bridging and bidentate ones). This result may seem in contrast with experimental works, which conclude with a bidentate conformation[70] or to a bridging adsorption[73] of carboxylic acids on oxidized aluminum. However, the studied surfaces exhibit different local structures than α-alumina. From our results, it appears that both the Al−Al distance at the surface and the Al coordination number will determine the binding mode (we showed here that bridging is favored on two Al_{III} but not on a $Al_{III}-Al_{IV}$ couple). The Al−Al distance is rather high on α-(0001) Al_2O_3 (4.80 Å), explaining why the bridging mode is not favored, but it is shorter on the (110) γ-Al_2O_3 surface (3.03 Å), and on the basal plane of boehmite (3.18 Å), which could be considered as alternative models of the oxidized aluminum surface. In addition, the (110) γ-Al_2O_3 surface exhibits Al_{III} atoms, which could favor a bridging configuration more than

the saturated Al_{VI} atoms on the boehmite (010) surface or the long distance $Al_{III}-Al_{III}$ in α-(0001) Al_2O_3. Although the present results cannot be directly extrapolated to other alumina surfaces, they provide clear conclusions that may help to predict the adsorption mode of glycine—or more generally of carboxylate-containing molecules.

The role of the carboxylate function has also been reported in studies of carboxylic acid adsorption on rutile TiO_2 surfaces,[74−76] where a bridging mode was invoked. Several theoretical studies propose a multidentate adsorption mode of COOH groups on TiO_2 surfaces.[24,59,61,62,74,77,78] Previous experimental studies[25,26] also report that glycine interacts preferentially via the COOH group with the TiO_2 surface. The Ti−Ti distance in rutile (2.97 Å) is compatible with the O−O distance (2.29 Å) in the carboxylate group, which explains the preferential bridging adsorption mode on rutile.

In contrast, the adsorption of glycine on silica seems to be driven by a different mechanism: recent experimental and theoretical data on silica conclude on the role of hydroxyl nests, and no Si−OC bond could be experimentally or theoretically evidenced.[5−6,12]

Regarding the nature of the conformer and the orientation of adsorbed glycine to the surface, our results illustrate the complexity and interplay of events that may lead to a given configuration. It appears that both the mode of binding with Al atoms and the H-bond network determine the orientation of glycine with respect to the surface and its final form (NG, ZG, or AG). Even on a small molecule such as glycine, it is found that the cooperation between Al−OC and H bonds may lead to nearly isoenergetic but different configurations of adsorption on the O_3Al termination (perpendicular anionic unidentate, parallel zwitterion unidentate, and parallel anionic bridging). In contrast to the O_3Al surface, on the hydroxylated surface, in order to maximize the number of H bonds with the surface, the parallel unidentate mode of adsorption is the most favored. Again, the ZG and AG forms are stabilized by a combination of an iono-covalent Al−OC bond and H bonds. Depending on the H network, and more precisely on the presence of water adsorbed on the surface, a proton transfer may occur from glycine to the neighbor water molecule, resulting in the stabilization of a glycinate and a solvated proton, stabilized by the basic hydroxyls at the surface. This is not possible in the absence of the adsorbed water molecule. In other words, a coadsorbed water molecule increases the basic character of the μ_1−OH group, which is able to trap the proton from the amine group.

The substitution of an OH group by glycine is favored thermodynamically. In other words, glycine tends (at least thermodynamically) to dehydroxylate the surface and to adsorb in place of water. Such a trend was already observed experimentally on TiO_2, where water is nondissociatively chemisorbed on the surface.[2] This may have an influence on the surface Al dissolution in water.

Conclusions

The main criteria governing the interaction of glycine with the (0001) α-alumina surface are the coordination number of the Al surface atom, the degree of hydroxylation of the surface, and the structural Al−Al distances at the surface. Depending on these parameters, the adsorption may be rather weak, forming a H-bond network that promotes a parallel adsorption on the surface (E_{ads} = 70 kJ/mol), or may involve an iono-covalent Al−OC bond(s) and thus a stronger interaction: On the OH-free oxide surface, an anionic form with a perpendicular orientation is the most stable form; on the hydroxylated surface, the parallel adsorption is favored, and when an Al−OC bond may be formed, the AG and ZG forms are isoenergetic. The substitution of a surface OH group by glycine is thermodynamically favored. Water coadsorption has a stabilizing effect.

Acknowledgment. Financial support from the GDR 2614 IFREMER-DGA-CNRS "Biosalissures Marines" is gratefully acknowledged. We also acknowledge the use of the computing resources provided by MOTT2 (EPSRC Grant GR/S84415/01, UK), the national IDRIS Center, and the Centre Calcul Recherche (CCR), University P. et M. Curie, Paris, France.

References and Notes

(1) Soria, E.; Román, E.; Williams, E. M.; de Segovia, J. L. *Surf. Sci.* **1999**, *543*, 433−435.
(2) Qiu, T.; Barteau, M. A. *J. Colloid Interface Sci*. **2006**, *303*, 229.
(3) Lausmaa, J.; Lofgren, P.; Kasemo, B. *J. Biomed. Mater. Res.* **1999**, *44*, 227.
(4) Meng, M.; Stievano, L.; Lambert, J.-F. *Langmuir* **2004**, *20*, 914.
(5) Lomenech, C.; Bery, G.; Costa, D.; Stievano, L.; Lambert, J-F. *Chem. Phys. Chem* **2005**, *6*, 1061.
(6) Stievano, L.; Lopes, I.; Piao, L-Y.; Meng, M.; Costa, D.; Lambert, J. F. *J. Eur. Miner*., in press.
(7) Tzvetkov, G.; Koller, G.; Zubavichus, Y.; Fuchs, O.; Casu, M. B.; Heske, C.; Umbach, E.; Grunze, M.; Ramsey, M. G.; Netzer, F. P. *Langmuir* **2004**, *20*, 10551.
(8) Fleming, G. J.; Idriss, H. *Langmuir* **2004**, *20*, 7540.
(9) Rimola, A.; Tosoni, S.; Sodupe, M.; Ugliengo, P. *Chem. Phys. Chem* **2006**, *7*, 157.
(10) Gambino, G. L.; Lombardo, G. M.; Grassi, A.; Marietta, G. *J. Phys. Chem. B* **2004**, *108*, 2600.
(11) Langel, W.; Menken, L. *Surf. Sci.* **2003**, *538*, 1.
(12) Rimola, A.; Sodupe, M.; Tosoni, S.; Civalleri, B.; Ugliengo, P. *Langmuir* **2006**, *22*, 6593.
(13) Costa, D.; Lomenech, C.; Meng, M.; Stievano, L.; Lambert, J-F. *J. Mol. Struct*.: *THEOCHEM* **2007**, *806*, 253.
(14) Costa, D.; Tougerti, A.; Tielens, F.; Gervais, C.; Lopes, I.; Stievano, L.; Lambert, J-F. To be submitted for publication.
(15) Maurice, V.; Marcus, P. Structure of Thin Anodic Films Formed on Single Crystals Metal Surfaces. *Interfacial Electrochemistry: Theory, Experiment, and Applications*; Marcel Dekker: New York, 1999; pp 541−558.
(16) van den Brandt, J.; Sloof, W. G.; Terryn, H.; de Wit, J. H. W. *Surf. Interface Anal.* **2004**, *36*, 81.
(17) van den Brandt, J.; Snijders, P. C.; Sloof, W. G.; Terryn, H.; de Wit, J. H. W. *J. Phys. Chem. B* **2004**, *108*, 6017.
(18) Alexander, M. R.; Beamson, G.; Bailey, P.; Noakes, T. C. Q.; Skeldon, P.; Thompson, G. E. *Surf. Interface Anal.* **2003**, *35*, 649.
(19) Wefers, K.; Misra, C. *Oxides and Hydroxides of Aluminum*, Alcoa Technical Paper N°19; Alcoa Technical Center: Alcoa, PA, 1987.
(20) Brady, M. P.; Brindley, W. J.; Smialek, J. L.; Locci, I. E. *J. Metals* **1996**, *48*, 46.
(21) Escuderoa, M. L.; Mun oz-Morrisb, M. A.; Garcy a-Alonsoa, M. C.; Fernandez-Escalantea, E. *Intermetallics* **2004**, *12*, 253.
(22) Gan, Y. Y.; Franks, G. V. G. V. *Langmuir* **2006**, *22*, 6087.
(23) Wolverton, C.; Hass, K. C. *Phys. Rev. B* **2000**, *63*, 024102.
(24) Ahuja, R.; Osorio-Guillen, J. M.; Souza de Almeida, J.; Holm, B.; Ching, W. Y.; Johansson, B. *J. Phys.: Condens. Matter.* **2004**, *16*, 2891.
(25) Pinto, H. R.; Nieminen, R. M.; Elliott, S. D. *Phys. Rev. B* **2004**, *70*, 125402.
(26) Mattson, A. E.; Jennison, D. R. *Surf. Sci*. **2002**, *520*, 611.
(27) Ruberto, R.; Yourdashahyan, Y.; Lundqvist, B. I. *Phys. Rev. B* **2003**, *67*, 195412.
(28) Ahn, J.; Rabalais, J. W. *Surf. Sci.* **1997**, *388*, 121.
(29) Coustet, V.; Jupille, J. *Nuovo Cimento* **1997**, *19*, 1657.
(30) Liu, P.; Kendelewicz, T. E. B. G.; Nelson, E. J.; Chambers, S. A. *Surf. Sci.* **1998**, *417*, 53.
(31) Elam, J. W.; Nelson, C. E.; Cameron, M. A.; Tolbert, M. A.; George, S. M. *J. Phys. Chem. B* **1998**, *102*, 7008.
(32) Kelber, J. A.; Niu, C. Y.; Shepherd, K.; Jennison, D. R.; Bogicevic, A. *Surf. Sci.* **2000**, *446*, 76.
(33) Saw, K. G. *J. Mater. Sci.* **2004**, *39*, 2914.
(34) O'Brien, W. L.; Jia, J.; Dong, Q.-Y.; Callcott, T. A.; Mueller, D. R.; Ederer, D. L.; Kao, C.-C. *Phys. Rev. B* **1993**, *47*, 15482.
(35) Eng, P. J.; Trainor, T. P.; Brown, G. E., Jr.; Waychunas, G. A.; Newville, M.; Sutton, S. R.; Rivers, M. L. *Science* **2000**, *288*, 1029.
(36) Henderson, M. A. *Surf. Sci. Rep.* **2002**, *46*, 5.
(37) Al-Abadleh, H. A.; Grassian, V. H. *Surf. Sci. Rep.* **2003**, *52*, 63.

(38) Guo, J.; Ellis, D. E.; Lam, D. J. *Phys. Rev. B* **1992**, *45*, 13 647.
(39) Wang, X. G.; Chaka, A.; Scheffler, M. *Phys. Rev. lett.* **2000**, *84*, 3650.
(40) Lodziana, Z.; Norskov, J. K.; Stoltze, P. *J. Chem. Phys.* **2003**, *118*, 11179.
(41) Gan, Y.; Franks, G. V. *J. Phys. Chem. B* **2005**, *109*, 12474.
(42) Perdew, J. P.; Wang, Y. *Phys. Rev. B* **1992**, *45*, 13244.
(43) DalCorso, A.; Pasquarello, A.; Baldereschi, A.; Car, R. *Phys. Rev. B* **1996**, *53*, 1180.
(44) Kresse, G.; Hafner, J. *Phys. Rev. B* **1994**, *49*, 14251.
(45) Kresse, G.; Furthmüller, J. *Comput. Mater. Sci.* **1996**, *6*, 15.
(46) Hafner, J. http://cms.mpi.univie.ac.at/vasp/.
(47) Kresse, G.; Joubert, D. *Phys. Rev. B* **1999**, *59*, 1758.
(48) Digne, M.; Sautet, P.; Raybaud, P.; Euzen, P.; Toulhoat, H. *J. Catal.* **2002**, *211*, 1.
(49) Bader, R. F. W. *Atoms in Molecules. A Quantum Theory*; Oxford University Press: New York, 1990.
(50) http://theory.cm.utexas.edu/vtsttools/bader/.
(51) Henkelman, G.; Arnaldsson, A.; Johnsson, H. *Comput. Mater. Sci.* **2006**, *36*, 354.
(52) Diawara, B. To be submitted for publication.
(53) Toebbens, D. M.; Stuesser, N.; Knorr, K.; Mayer, H. M.; Lampert, G. *Mater. Sci. Forum* **2001**, *378*, 288.
(54) Hector, L. G., Jr.; Opalka, S. M.; Nitowski, G. A.; Wieserman, L.; Siegel, D. J.; Yu, H.; Adams, J. B. *Surf. Sci.* **2001**, *494*, 1.
(55) Stepanian, S. G.; Reva, I. D.; Radchenko, E. D.; Rosado, M. T. S.; Duarte, M. L. T. S.; Fausto, R.; Adamowicz, L. *J. Phys. Chem. A* **1998**, *102*, 1041.
(56) Aikens, C. M.; Gordon, M. S. *J. Am. Chem. Soc.* **2006**, *128*, 12835.
(57) Tasker, P. W. *Adv. Ceram.* **1984**, *10*, 176.
(58) Hass, K. C.; Schneider, W. F.; Curioni, A.; Andreoni, W. *J. Phys. Chem. B* **2000**, *104*, 5527.
(59) Ramaekers, R.; Pajak, J.; Lambie, B.; Maes, G. *J. Chem. Phys.* **2004**, *120*, 4182.
(60) We envisaged also the transfer of an acid proton (H from μ_3-OH) from the surface to glycine, following $Al_3O{-}H + NG \rightarrow Al_3O + CG$, where CG is the cationic conformer of glycine, but the CG configugation was found to be not stable, resulting in a spontaneous transformation into NG.
(61) Digne, M. P.; Sautet, P. P.; Raybaud, P.; Euzen, P.; Toulhoat, H. *J. Catal*. **2004**, *226*, 54.
(62) Mercero, J. M.; Fowler, J. E.; Ugalde, J. M. *J. Phys. Chem. A* **1998**, *102*, 7006.
(63) Costa, D.; et al. To be submitted for publication.
(64) Digne, M.; Sautet, P.; Raybaud, P.; Euzen, P.; Toulhoat, H. *J. Catal.* **2004**, *226*, 54.
(65) This value was calculated after optimization of the same configuration in absence of the water molecule (ZG/alumina), following the reaction $(ZG + H_2O)/alumina \rightarrow ZG/alumina + H_2O_{gas}$, and $\Delta E_{ads} = E(ZG/alumina) - E((ZG + H_2O)/alumina) - E(H_2O_{gas})$.
(66) Rosenqvist, J.; Axe, K.; Sjöberg, S.; Persson, P. *Colloids Surf., A* **2003**, *220*, 91.
(67) Yoon, T. H.; Johnson, S. B.; Brown, G. E., Jr. *Langmuir* **2005**, *21*, 5002.
(68) van den Brand, J.; Blajiev, O.; Beentjes, P. C. J.; Terryn, H.; de Wit, J. H. W. *Langmuir* **2004**, *20*, 6318.
(69) Hall, J. T.; Hansma, P. K. *Surf. Sci.* **1978**, *76*, 61.
(70) Kiselev, A. V.; Uvarov, A. V. *Surf. Sci.* **1967**, *6*, 399.
(71) Yoon, T. H.; Johnson, S. B.; Musgrave C. B.; Brown, G. E., Jr. *Geochim. Cosmochim. Acta* **2004**, *22*, 4505.
(72) Yoon, T. H.; Johnson, S. B. Brown, G. E., Jr. *Langmuir*, **2005**, *21*, 5002.
(73) van den Brand, J.; Blajiev, O.; Beentjes, P. C.; Terryn, H.; de Wit, J. H. W. *Langmuir* **2004**, *20*, 630.
(74) Patthey, L.; Rensmo, H.; Persson, P.; Westermark, K.; Vayssieres, L.; Stashans, A.; Pertersson, Å.; Brühwiler, P. A.; Siegbahn, H.; Lunell, S.; Mårtensson, N. *J. Chem. Phys.* **1999**, *110*, 5913.
(75) Schnadt, J.; O'Shea, J. N.; Patthey, L.; Scheissling, J.; Krempaský, J.; Shi, M.; Mårtensson, N.; Brühwiler, P. A. *Surf. Sci.* **2003**, *544*, 74.
(76) Ojamae, L.; Aulin, C.; Pedersen, H.; Kall, P. O. *J. Colloid Interface Sci.* **2006**, *296*, 71.
(77) Sushko, M. L.; Gal, A. Y.; Schluger, A. L. *J. Phys. Chem. B* **2006**, *110*, 4853.
(78) Fahmi, A.; Minot, C.; Fourré, P.; Nortier, P. *Surf. Sci*. **1995**, *343*, 261.